Atomic Clocks Research in The Aerospace Corporation Chemistry and Physics Laboratory -- An Overview

R. P. Frueholz, N. D. Bhaskar, J. C. Camparo,
B. Jaduszliwer, and C. M. Klimcak

Chemistry and Physics Laboratory
The Aerospace Corporation
P. O. Box 92957, Los Angeles, CA 90009

Abstract

One role of The Aerospace Corporation is to act as a source of technical and scientific expertise for its principal customer, the United States Air Force Space Division. In support of this role the Corporation's Chemistry and Physics Laboratory conducts a research program investigating various aspects of atomic frequency standards. The prime objective of the program is to improve the reliability and performance of the atomic frequency standards used on Air Force satellites. In meeting this objective the investigations maintain broad expertise across the range of traditional standards, rubidium and cesium, as well as developing expertise in standards with potential satellite applications, for example the hydrogen maser and the stored-ion standard. Several areas associated with improving the performance and reliability of the rubidium standard are under investigation: analytical modelling of clock frequency stability, the origins of frequency drift, advanced, laser-based optical pumping techniques, and discharge lamp reliability. Our prime concern with the cesium standard involves improving the reliability of compact, satellite compatible designs. Topics currently being studied include: graphite gettering of expended cesium, electron multiplier gain decay processes, and cesium oven performance. Investigations aimed at improving hydrogen maser performance include study of the motional narrowing process which yields the narrow hyperfine resonance feature upon which maser operation is based and characterization of hydrogen dissociator performance in terms of hydrogen consumption and the velocity distribution of the emitted hydrogen atoms. It is anticipated that the detailed descriptions of these studies presented in this paper will further inform the time and frequency community of the capabilities of Aerospace's Chemistry and Physics Laboratory and promote the efficient exchange of information between our laboratory and both government and commercial organizations.

I. INTRODUCTION

One role of The Aerospace Corporation is to act as a source of technical and scientific expertise for its principal customer, the United States Air Force Space Division. In support of this role the Corporation's Chemistry and Physics Laboratory (CPL) conducts a research program investigating various aspects of atomic frequency standards. The prime objective of the program is to improve the reliability and performance of the atomic frequency standards used on Air Force satellites. In meeting this objective the investigations maintain broad expertise across the range of traditional standards, rubidium (Rb) and cesium (Cs), as well as developing expertise in standards with potential satellite applications, for example the hydrogen (H) maser and the stored-ion standard. In this paper, an overview of The Aerospace Corporation's CPL Atomic Clock Research Program is presented.

One factor distinguishing the work being conducted at Aerospace from that being carried out at other laboratories as well as by clock manufacturers is that complete clock prototypes are not fabricated. In contrast, our efforts are directed toward very specific aspects of the various standards designed for satellite use. Satellite standards must satisfy stringent requirements not normally applied to standards designed for commercial use or even earth-based military applications. Foremost among these special requirements is extreme reliability and longevity. Additionally, high performance must be obtained within the constraints of limited size, weight, and power consumption. With these specialized requirements in mind, various areas of investigation are selected. The main areas of expertise of the research staff are physics and chemistry. When performing studies, heavy emphasis is placed on understanding the underlying chemistry and physics associated with the area of investigation. In our experience, initially developing this fundamental understanding results in the highest long term productivity. As will be apparent in the detailed discussions of current investigations this philosophy is applied to virtually all areas of study.

To introduce the CPL Atomic Clocks Program, topics currently under investigation are shown on Fig. 1. These topics are broken down by the specific frequency standard they affect most directly as well as indicating whether they primarily impact the standard's reliability or performance capabilities. Currently, Global Positioning System (GPS)/NAVSTAR satellites use both Cs and Rb standards while advanced communication systems will utilize Rb standards. Consequently, in our program heavy emphasis is placed on improving the reliability of these devices and understanding the physical processes which limit their ultimate frequency stabilities. A significant amount of effort has been expended developing a theoretical model of Rb clock performance. The model yields the frequency stability of the standard as a function of the physics package geometry and easily measured parameters. An undesirable trait of the Rb standard is the characteristic drift of output frequency. One goal of our Rb standard studies is to understand the origin of frequency drift and reduce its magnitude. Since optical pumping is the process which allows effective detection of the Rb hyperfine resonance frequency we are investigating the physical processes which limit its efficiency and hence frequency standard short term stability.

Studies associated with the Cs standard center on improving the reliability of compact, satellite compatible designs. Graphite is typically employed to remove spent Cs within beam tubes. Saturation of this getter material can result in standard failure. We are determining minimum amounts of graphite needed to absorb specific amounts of Cs as well as the optimum type of graphite and processing procedure. Additionally, the causes of electron multiplier gain decay, a commonly observed process in Cs beam tubes, are being investigated. A final area of investigation deals with the performance of the Cs oven. Efficient use of Cs is particularly important in ensuring adequate standard lifetime. Techniques have been developed to characterize the performance of these ovens in terms of the angular distributions of Cs atoms emitted from them.

Hydrogen masers are being considered for use on future GPS satellites. Two areas of investigation are directed toward improving H-maser performance: motional narrowing, which is the process that yields the extremely narrow H-atom hyperfine resonance observed in the maser, and hydrogen dissociator performance which supplies the atomic H required by the maser. In the area of motional narrowing, experiments have been initiated to confirm the accuracy of a new theoretical technique for computing these lineshapes. With regard to dissociator performance, it should be appreciated that only a small fraction of the emitted atoms have useful velocities and that very little information concerning the velocity distributions is available. We have completed construction of an apparatus capable of analyzing the performance of various dissociator designs in terms of overall efficiency and the velocity distributions of the emerging H-atoms. Our ultimate objective is to increase the usable fraction of atoms leaving the H-dissociator, reducing both the amount of H required during the standard's lifetime and the total H pumping capacity. Attainment of our objective will lead to a more reliable space standard.

The body of the paper will discuss in greater detail the projects currently in progress in The Aerospace Corporation's CPL. Emphasis will be placed on indicating the relevance of each project to the stated objectives as well as providing summaries of our most recent results. It is hoped that the following summaries will further inform the time and frequency community of the capabilities of the Aerospace's CPL and promote the efficient exchange of information between our laboratory and both government and commercial organizations.

II. DESCRIPTION OF AREAS OF INVESTIGATION

A. Studies Related to the Rubidium Standard

1. The Aerospace Rubidium Clock Performance Model

Over the past several years we have maintained a concentrated effort developing and exploiting a non-empirical model of the gas cell atomic frequency standard; specifically a model that: 1) is reasonably accurate in predicting clock performance as specified by the Allan variance, 2) is valid for both short and long averaging times, 3) is general enough so as to apply to gas cell standards based on alkalies other than Rb e.g. Cs, and 4) does not

require any measurements of clock signal characteristics. Consistent with our approach to research, before even attempting to develop a clock model, our initial work was aimed at understanding the 0-0 hyperfine transition lineshape in optically pumped alkali metal vapors. These initial studies, analyzing the basic physics occurring within the clock, showed that the theory of the Rb hyperfine transition lineshape as originally developed by Vanier[1] was quite accurate in its predictions, and that it could also be generalized to alkali atoms with arbitrary half-integer nuclear spin.[2] The resulting "Generalized Vanier Theory" has thus formed the basis of our non-empirical clock model. We anticipate that this clock model will find application in the analysis of design tradeoffs for specific applications, that it will be employed to diagnose clock parameters that limit performance, and that is will also prove useful in suggesting the most promising avenues for future frequency standard improvement.

In brief, our model of the gas cell standard considers the relevant physics as occurring on two different scales.[3] On the microscopic scale the 0-0 hyperfine transition lineshape is determined by the Generalized Vanier Theory of alkali atom hyperfine optical pumping. Among other parameters, this theory considers the dependence of the hyperfine lineshape on optical pumping light intensity and microwave Rabi frequency. However, because the buffer gas pressure in a typical gas cell standard effectively freezes the atoms in place on the time scales of the order of a Rabi period,[4] and because the alkali vapor is not necessarily optically thin, these two parameters vary from atom to atom within the vapor. Furthermore, as a result of diffusion to the resonance cell's walls, where the atoms immediately depolarize on impact, there is a spatial distribution of hyperfine polarization.[5] In some sense this spatial distribution of hyperfine polarization can be imagined as being superimposed on the microscopic physics. Thus, there is a macroscopic scale of physics in the problem which is related to the spatial variations of (a) the optical pumping light intensity, (b) the microwave Rabi frequency, and (c) the hyperfine polarization as a result of diffusion to the resonance cell walls.

In order to treat this macroscopic scale of physics in a reasonably lucid manner, the problem is reduced to one dimension, so that only the longitudinal variation of the optical pumping light intensity and microwave field strength is considered. The microwave Rabi frequency axial distribution is determined by the microwave cavity mode. The axial variation of the optical pumping light intensity is determined by computing a "global" optical pumping parameter. In essence this global optical pumping parameter determines the fractional population in the optically absorbing hyperfine multiplet, and thus the optical depth of the vapor as a result of optical pumping. Since we assume that the atoms are effectively frozen in place as a result of the buffer gas, the first order change in transmitted light intensity as a function of microwave Rabi frequency, for a uniform slice of vapor of infinitesimal thickness dz, only depends on the local values of the optical pumping light intensity and microwave Rabi frequency. In order to include the effects of diffusion, this first order macroscopic solution is then multiplied by an envelope function which describes the axial distribution of hyperfine polarization in an optically thin vapor. Once the clock signal lineshape is calculated, it is a straightforward task to determine the clock's error signal, and hence its stability as specified by the Allan variance.

At this point our ability to model the performance of Rb clocks and gas cell standards in general is quite mature. In addition to the calculation of short term frequency stability just discussed, techniques have been developed to model long term frequency stability. This is accomplished by considering noise sources other than lamp induced shot noise.[3] It is our hope that the clock model will eventually be of use to Rb clock manufacturers allowing more rapid analysis of potential performances of various clock designs.

Recently, we have employed our model in explorations of two promising areas of gas cell frequency standard improvement. In our first series of calculations we considered the improvement in short term performance that could result from diode laser optical pumping.[6] Our results showed that, whereas in present gas cell standards shot noise limits the short term stability,[7] in a diode laser pumped clock laser quantum noise would limit the ultimate frequency stability that could be attained. However, if one can reduce the laser quantum noise, for example by using an enhanced cavity Q diode laser, one could potentially achieve short term stabilities approaching $6 \times 10^{-15}/\sqrt{\tau}$. In our second series of calculations we considered gas cell standards based on alkalies other than Rb.[8] In particular we were interested in exploring the expected short term stability of a Cs gas cell standard. Surprisingly, our calculations indicated that a Rb^{87} gas cell standard shows the greatest potential for short term frequency stability, even though Cs has the greater ground state hyperfine splitting. Additionally, these calculations indicated the importance of microwave cavity geometry on the stability one can attain with gas cell standards. With the conclusion of these exploratory calculations into gas cell standard improvement, we have shifted our application of the clock model into the area of diagnosis. Specifically, we are attempting to understand the mechanism(s) of frequency drift in the Rb gas cell standard.

2. Frequency Drift in the Rubidium Standard

Uncorrected frequency drift in the Rb vapor atomic frequency standard can be a significant source of time error for systems based on this standard. On GPS satellites, Rb frequency drift so impairs the standard's timekeeping ability that the heavier Cs standards are now employed as the principal time keeping devices. The reduction or elimination of frequency drift could allow the Rb standard to play a more active role in satellite based timekeeping, with a potential reduction in total clock weight on the satellite. Unfortunately at this point, not only are the origins of this drift not well understood, but its characteristics have not been fully documented. In CPL the origins of frequency drift in the Rb standard have recently begun being investigated. Our initial studies have approached the subject at a very fundamental level. As a first step in understanding drift we reviewed the available experimental data, and arrived at a consistent set of general Rb clock drift characteristics:[9] 1) on an individual standard the sign of the drift coefficient may be variable; 2) the magnitude and sign of the drift coefficient are typically only stable over a period of roughly three months, and 3) the general Rb clock drift coefficient is $(5 \pm 2) \times 10^{-12}$/ month. Using these characteristics, we then considered eleven basic physical mech-

anisms capable of inducing drift, and found that only four of the mechanisms were consistent with the characterization:[9] 1) a temperature-induced pressure shift mechanisms, 2) a quadratic Zeeman shift mechanisms, 3) a spectrum dependent light shift mechanisms, and 4) a position shift mechanism. We now plan to analyze these four plausible mechanisms of drift in much more detail using a modified version of our clock model. This model will differ from the one employed previously in that it will be a three dimensional model of the clock, and will incorporate various inhomogeneous frequency shift phenomena (i.e., the position shift effect[10] and the inhomogeneous light shift effect[11,12]). It is anticipated that application of this model will shed light on the mechanism(s) of drift in the Rb gas cell atomic frequency standard.

3. Optical Pumping of Zeeman Level Populations

As is well known optical pumping is a process by which nonthermal equilibrium population distributions among atomic energy levels (and sublevels) are obtained by the interaction of light with an ensemble of atoms.[13] In the Rb vapor frequency standard this process used to generate hyperfine polarization in the atomic ground state using isotopically filtered light. Since only a small fraction of the atoms thus optically pumped (only atoms in the m_F=0 Zeeman sublevel of each hyperfine level) are utilized for generating the microwave clock signal, the atoms in the $m_F \neq 0$ Zeeman sublevels are essentially "wasted". Thus, a clock in which nearly all of the atoms are pumped into one of the two m_F=0 sublevels would exhibit a greater signal-to-noise ratio and hence improved performance (see Fig. 2).

This, however, is a non-trivial problem, and in order to accomplish this we need to address several issues of basic importance.[14]

a) The dependence of the Zeeman sublevel population distribution on the characteristics of the pumping radiation (e.g., frequency and polarization) and the role of the excited state in determining the ground state distribution.

b) The role of relaxation processes which tend to restore thermal equilibrium in the ensemble. In particular the effect of spin exchange collisions on the population distribution needs careful examination.

c) Dynamic transformations of population distributions using combinations of microwave and radio frequency fields.

In brief, our goal is to customize the ground state population distribution among the Zeeman sublevels allowing development of gas cell standards with improved frequency stabilities. Consequently, we have started a comprehensive program to study these and related issues. Specifically, we have developed the necessary experimental technique to characterize the atomic population distribution among the ground state Zeeman sublevels for different optical pumping conditions.

The schematic of the optical pumping apparatus is shown in Fig. 3. A small spherical glass cell containing a mixture of Rb vapor and different

buffer gases (N_2 and He) is placed at the center of a pair of Helmholtz coils. Circularly polarized D_1 light (794.7 nm) is used to optically pump the Rb vapor. In this configuration, the optical pumping process is used to spin polarize the Rb vapor. Due to the strong hyperfine coupling a significant electronic and nuclear polarization of the Rb vapor is achieved. This results in an unequal population distribution among the Zeeman sublevels of each hyperfine level. The details of the population distribution are determined by various rates: optical pumping, spin exchange and spin relaxation. A radio frequency magnetic field oscillating at right angles to the static field is used to induce $\Delta m_F = \pm 1$ transitions between the Zeeman sublevels of each ground state hyperfine level. Radio frequency resonance is detected as the change in intensity of the transmitted light reaching the photodetector. At sufficiently high D.C. magnetic fields (> 15 gauss) all the individual Zeeman transitions are well resolved. The frequency of the rf magnetic field is fixed while the D.C. magnetic field is slowly scanned. The energy splitting between the Zeeman sublevels is given by the Breit-Rabi formula in the range of intermediate external magnetic fields.[15]

Typical experimental results of the radio frequency spectra scanning all the Zeeman transitions are shown in Fig. 4. For Rb^{85} which has nuclear spin 5/2, the signal consists of ten well resolved transitions whereas Rb^{87} (not shown) which has nuclear spin 3/2, gives rise to six transitions. For weak rf fields (well below saturation) and optically thin vapor conditions the signal amplitude is directly proportional to,

$$\Delta n = n(F,m_F) - n(F,m_F-1), \qquad (1)$$

with $n(F, m_F)$ the population of a particular Zeeman sublevel specified by the quantum numbers F and m_F. This is used to infer the general population distribution among the Zeeman levels. For the data shown here, the experimental conditions are characterized by the rates of spin exchange between Rb atoms being larger than all the other relevant rates in the system. This corresponds to a situation in which the Zeeman population distribution is characterized by a spin temperature.[16] Quantitatively, the state population is given by $n_i = Ce^{-n_i\beta}$, where n_i is the population of the ith ground state sublevel and β is determined by the total polarization of the sample.

In these initial investigations we have clearly demonstrated the effectiveness of radio frequency resonance spectroscopy for studying the relative population distributions in optically pumped Rb vapors. Experiments are in progress to study the relative population distribution when the vapor is optically pumped with a tunable laser. The ultimate goal of these studies, of course, is the development of optical pumping techniques which will yield lightweight gas cell standards displaying frequency stabilities much better than are currently available. With the advent of tunable diode lasers as sources of optical pumping radiation this appears feasible. All of the results of these investigations will be available to the general clock community, it is our hope that these studies will lay the foundation for the "next generation" of gas cell standards.

4. Rubidium Discharge Lamp Reliability

For the past several years our laboratory has been involved in a variety of studies concerning the lifetime and reliability of the discharge lamps that are used in Rb frequency standards. Failure of these lamps was the major cause of failure of Rb standards on GPS satellites. Our experimental investigations have enabled us to develope a quantitative model of lamp failure that can be used to predict the lifetime of newly manufactured discharge lamps.[17] This model is derived from our attempts to form a basic understanding of the physical processes that impact lamp reliability. The success of this model has allowed us to provide recommendations to lamp manufacturers concerning the lamp glass composition and the initial Rb fills that will insure reliable lamp operation and hence Rb standard operation.

The primary failure mechanism of the lamps has been shown to be caused by the diffusion of Rb into the glass envelope. This conclusion was made after conducting a study of the rate of consumption of free metallic Rb in a large collection of operating discharge lamps. The amount of Rb consumed was extracted from measurements of the mass of free Rb remaining in the lamps at several stages during their operating history. This mass was obtained from calorimetric measurements of the thermal energy that was required to melt the free Rb in the lamp.[18] The amount of Rb consumed by the lamps exhibited a dependence on lamp operating time t that displayed the characteristic $t^{1/2}$ signature of a diffusional loss process. A typical consumption curve is shown in Fig. 5.

Our consumption data has been fitted to a modified diffusion model that incorporates an initial reaction loss mechanism. The initial loss is presumably due to the gettering action of impurities that are inadvertently introduced by the lamp manufacturer. The form of the consumption law predicted by our model is:

$$M_{Rb}(t) = R\sqrt{t} + B, \qquad (2)$$

with $M_{Rb}(t)$ the mass of Rb consumed as a function of lamp operating time. R and B are parameters determined from experimental consumption data. The prediction of our model for the particular lamp of Fig. 5 is indicated by the solid line. Similar agreement was obtained for the remaining lamps in our study.

The calorimetric technique of Rb measurement, first demonstrated by the Rb clock team of EG&G's Electron Devices Group, together with the fundamental understanding of Rb-glass interactions developed at Aerospace have significantly improved the reliability of Rb standards. We believe that these techniques could be employed in conjunction with an initial, short-term measurement program to further insure the lifetime of newly manufactured lamps. This form of quality control would present an effective screen against premature lamp failures due to production anomalies. Increased reliability would result from these efforts.

B. Studies Related to the Cesium Standard

Cesium beam atomic frequency standards are used on board NAVSTAR/GPS satellites because of their excellent frequency stability and virtually non-existent frequency drift. Stable operation of GPS-type Cs beam clocks is achieved by locking the output of a voltage-controlled quartz-crystal oscillator (VCXO) to the Cs (F=3, M=0) $\leftrightarrow$ (F=4, M=0) hyperfine transition at frequency $f_o \cong 9.2$ GHz. The Cs beam is interrogated by microwaves synthesized from the VCXO and frequency (or phase) modulated at a frequency f which is a significant fraction of the atomic transition linewidth. If the microwave mean frequency deviates from f_o, the atomic beam becomes amplitude-modulated at the frequency f. The beam component at the modulation frequency f is detected synchronously with the modulation to provide the error signal for the electronic servo loop that locks the VCXO to the atomic transition. In GPS-type Cs beam tubes (CBTs) the atoms are state-selected prior to, and state-analyzed after microwave interrogation by inhomogeneous field magnets; they are detected by surface ionization on a hot wire followed by amplification in an electron multiplier (EM).

1. Performance Related Areas of Analysis

A wide range of physical processes impact the frequency stability of the Cs standard. In our analysis of this device we have investigated several processes which determine how effectively synchronous detection can extract information from the amplitude modulated Cs atomic beam leaving the microwave interrogation region. Eventually, these investigations will form one section of a detailed model of Cs clock performance similar to that developed for the Rb standard. We have studied the impact of the statistical spread in atomic transit times and ionic residence times on the clock's performance. The distribution of ionic residence times on the hot wire is exponential, characterized by a temperature-dependent ionic dwell time τ, which is given for Cs ions on polycrystalline tungsten[19] in Fig. 6. As a result of this, the hot wire ionizer behaves in the frequency domain as a low-pass filter of cut-off frequency $f_I = 1/2\pi\tau$, thus setting an upper bound to the clock's modulation frequency. Since τ decreases with temperature, running the ionizer wire hotter allows higher modulation frequencies. The effect of the distribution of ionic residence times is to distort the amplitude-modulated atomic beam waveform, as shown in Fig. 7 for the case of f approximately 500 Hz and $\tau = 3 \times 10^{-4}$. An additional source of waveform distortion is the spread in atomic velocities leading to a distribution of transit times between the point of modulation and the detector. Fig. 8 shows the results for a gaussian velocity distribution with a mean velocity $\bar{v}$ of approximately 120 m/s and standard deviation $\sigma = 10$ m/s; the mean transit time is $\bar{t}_A = 1.4 \times 10^{-3}$ sec and $f \cong 500$ Hz. In GPS-type CBTs the state selecting and analyzing magnets transmit a narrow slice of the Maxwellian velocity distribution characteristic of the Cs atoms in the effussive beam. Increasing the width of the velocity distribution will on the one hand increase the beam intensity, and thus the clock's signal-to-noise ratio, and on the other hand will increase the waveform distortion, and thus reduce the clock's signal-to-noise ratio. Fig. 9 shows the combined results of these competing processes: it gives the signal-to-noise ratio vs. the width (expressed as a standard deviation) of a gaussian velocity

distribution of mean $\bar{v} \simeq 120$ m/s. Again, $\bar{t}_A = 1.4 \times 10^{-4}$sec $\tau = 3 \times 10^{-4}$ s and $f \simeq 500$ Hz. It can be seen that in this case there is an optimal width, 18 m/s.

2. Electron Multiplier Gain Decay Processes

Cesium beam tubes on board NAVSTAR/GPS satellites have displayed pronounced reductions in EM output current with operating time, which could affect the frequency stability of the clock and thus the system's performance. A likely cause of this reduction is EM gain degradation. Consequently we are investigating EM gain decay processes. Three possible modes of gain degradation are:

a) gain loss at the first dynode, due to surface changes caused by Cs ion impact or high Cs concentration;

b) surface deterioration due to electron impact, which would affect most seriously the last dynode gain, and

c) uniform gain degradation of all dynode surfaces, due to slow surface contamination.

A two-pronged study of this problem is in progress: the impact of EM gain degradation on the clock's frequency stability and its sensitivity to the site of degradation has been investigated theoretically. We also are conducting an experimental study of the long-term behavior of EM gain when it is used to detect Cs ions in conditions similar to those in operating CBTs, in order to identify the site within the multiplier of any observed gain degradation. The theoretical studies show that gain degradation will have relatively low impact on the clock's frequency stability when localized in the last dynode or uniformly distributed among all dynodes. Its impact will be worst when degradation is localized at the first dynode. In the latter case the white noise Allan variance amplitude will increase as the square root of the beam decay factor. Our experimental testing technique consists of bombarding the first dynode of an eight dynode GPS-type EM with a Cs ion beam of similar characteristics to the one in GPS CBTs. Output leads are provided for the first, second, seventh and eighth dynodes, as well as the anode. If I_i is the current collected by the i-th dynode and I_g is the anode current, $\delta_i = I_{i+1}/I_i$ gives the gain of the i-th dynode, while the overall gain is $G = I_g/I_1$. In this way the gain of the first and last dynodes, as well as the overall gain, can be monitored. Fig. 10 shows schematically our experimental setup, consisting of a conventional effusive Cs oven and graphite collimator, a hot-wire surface ionizer and einzel lens to extract and project the ion beam onto the first dynode of the EM under test. Graphite blocks are added at various positions to getter the Cs vapor, and a second hot-wire ionizer and ion collector monitor the background Cs vapor pressure. An EM has been monitored for about 300 days, and our results, some of which are shown in Fig. 11, indicate that the first dynode gain has not changed significantly except for the first few days of operation, and that the last dynode accounts for most of the overall gain degradation. These results should be taken "cum grano salis", since the multiplier was exposed to air for an unknown length of time

while in transit to The Aerospace Corporation. We are currently testing a second apparatus which will allow us to monitor up to four EMs simultaneously.

3. Cesium Gettering by Graphite

In Cs beam tube clocks only a small fraction of the Cs atoms effusing from the oven travel through the microwave cavity. A large fraction of the effusing atoms are gettered by slits and baffles made of graphite placed at various locations inside the clock. Should the graphite getters cease absorbing Cs, the increasing Cs background would rapidly obscure the true signal needed to operate the standard. Getter failure is then a life limiting process in the Cs clock. For the clock to be reliable the gettering lifetime should be at least as long as the required lifetimes of the tubes. This is of particular concern for standards used on satellites which must have at least 7.5 year lifetimes. Essentially no information concerning the amount or the type of graphite needed to absorb the oven's Cs charge is presently available.

We have been studying the gettering of Cs by graphite through the measurement of the sticking coefficient of Cs on graphite relative to a paraffin coated surface which is known to be perfectly nonsticking.[20] The experimental technique is illustrated in Fig. 12. A well collimated beam of Cs atoms is directed towards a graphite target. The reflected beam at a particular angle θ is measured using a hot-wire surface ionizer detector. The sticking coefficient γ is defined as,[21]

$$\gamma(\theta) = 1 - \frac{\text{reflected signal from graphite at } \theta^{\circ}}{\text{reflected signal from paraffin at } \theta^{\circ}} . \qquad (2)$$

We study the evolution of γ as a function of Cs exposure time and for various incident Cs atomic beam intensities. These experiments are carried out in an atomic beam apparatus operating at typical background pressures less than 1×10^{-8} torr.

Typical experimental results are shown in Fig. 13. The sticking coefficient starts at essentially unity, and declines with time, the rate of decline and the asymptotic values are both dependent on the incident beam intensities. One of the interesting results to emerge from our systematic studies is the dependence of the sticking coefficient on the vacuum processing of graphite prior to Cs exposure. High temperature baking of graphite in high vacuum is essential to good sticking coefficients. Another interesting aspect to emerge from our studies is the fact that after several days of exposure to Cs vapor the sticking coefficient essentially reaches an asymptotic value much less than unity. This has far reaching implications regarding the effectiveness of graphite in gettering Cs over long periods of time. Further experiments are planned to address this issue in greater detail.

The precision and reproducibility of our data is excellent, allowing theoretical analysis of the gettering process. Through this analysis we wish to develop means of predicting gettering capabilities after several years of Cs exposure. Finally, the greater sensitivity is being employed to study effects of different graphite surface conditions on gettering capabilities.

4. Cesium Oven Performance

Oven design is important to the operation of the Cs standard because the angular distribution of atoms effusing from the oven is a factor in determining the lifetime of the oven, and the intensity at the peak of the beam must be high enough to yield an adequate signal-to-noise ratio. Too much off-axis Cs could also shorten the life of the getters and contribute to background noise at the detector. Ovens used on satellites also must have acceptable heating power requirements. These constraints are somewhat different from those on laboratory atomic beam sources, and a different design philosophy is required.

To aid in designing Cs ovens for use in satellite compatible standards, an apparatus was constructed to measure the angular distribution of atoms effusing from Cs ovens. The apparatus is a simple modification of the system used to study graphite getter sticking coefficients. In this apparatus, shown schematically in Fig. 14a, the oven aperture sits at the center of rotation of a moveable surface ionization detector, mounted on a magnetic rotary motion feedthrough. The measured angular distributions are used to characterize the oven design performance. This is done by multiplying the measured distributions by the sine of the angle off the beam axis and integrating over all angles up to 90 degrees off axis. This integration gives a value for the total amount of material effusing from the oven for a given on-axis beam intensity. For application in an atomic clock, a good oven design must minimize the total amount of effusing material for a given beam intensity in order to conserve Cs and extend clock life. We compute a figure-of-merit (FOM) for an oven design by comparing the ratio of the beam intensity to the total effusate to the same ratio for an ideal "cosine" distribution oven. A cosine distribution is what theory predicts should be obtained for a hole in a very thin wall. Since a cosine distribution is the broadest possible distribution for effusion, it is the worst possible performance for an oven design, and will have an FOM of unity. Typical experimental results are shown on Fig. 14b. A particular strength of the apparatus is its ability to investigate angular distributions at large angles into which most of the Cs atoms are actually emitted. Thus far our apparatus has been used to study homebuilt ovens with FOMs near 5 and GPS-type ovens with much higher FOMs.

C. Studies Related to the Hydrogen Maser

Since its invention more than twenty years ago, the H maser has promised to be a source of very precise frequency and time information, in fulfillment of these expectations H masers have found a variety of applications. For the Air Force, H masers may be launched on GPS satellites, where atomic clock timing information allows very precise navigation anywhere on the Earth's surface or in its atmosphere. Additionally the H maser will certainly be a major component in future space systems, where extreme autonomy and survivability, attainable with the maser's superb frequency stability, are required. However, while these atomic devices will find an ever widening range of space applications, a detailed understanding of their various components' operating principles is not always available. Consequently, we are

investigating components with the goal of identifying and remedying characteristics which might hinder H maser application in future space systems.

1. Dicke Narrowing of the Hydrogen Hyperfine Resonance

The "heart" of the H-maser is a narrow atomic resonance ($Q_{atomic} \sim 10^9$) associated with the well known 21 cm line of hydrogen (see Fig. 15). This high atomic Q results from a process known as "Dicke-narrowing", where the Doppler shifts due to an H atom's motion are essentially averaged to zero as a result of collisions with the teflon coated walls of the H atom's storage vessel. Unfortunately, to date the phenomenon of Dicke-narrowing as it occurs in the H maser has not been well understood; and since atomic motion which doesn't average to zero robs useful signal from the maser, accurate signal-to-noise predictions of various H-maser designs have been lacking. Recent work in our laboratory, however, has shed new light on the Dicke-narrowing process. In particular, our studies indicate that when an atom impacts the coated surface it can scatter from the surface through one of two channels: a trapping-desorption (TD) channel, or a quasi-elastic (QE) channel. In brief, slow atoms scatter predominantly through the TD channel, while fast atoms scatter through the QE channel. Since our analysis shows that the narrow maser signal will only come from atoms which scatter through the QE channel, the ensemble of atoms contributing to the maser signal will necessarily be described by a temperature higher than thermal. Consequently, to understand Dicke-narrowing, allowing accurate calculation of the H-resonance lineshape, one needs to consider the higher effective temperature associated with the maser signal. These conclusions are particularly important to the development of an H maser theoretical signal model, which is intended to eventually predict signal-to-noise ratios and atomic Qs for various H-maser designs of interest for space applications.

2. Performance of the Hydrogen Dissociator

A critical component of the maser from the point of view of reliability and long-term operation is the source of atomic hydrogen, the H_2 dissociator. Its performance will determine the hydrogen budget of the maser, a good fraction of its power budget and the vacuum pumping requirements. The overall hydrogen efficiency of the maser is the ratio of the excess flow of atoms in the F=1, M=0 hyperfine state into the maser bulb (which is determined by the maser oscillation condition[22]), and the total hydrogen flow into the dissociator. This ratio will be determined partly by the atomic fraction in the dissociator outflow, and partly by the focussing properties of the state-selecting magnet. Since atomic deflection in an inhomogeneous magnetic field is inversely proportional to the square of the atomic speed, the atomic velocity distribution at the dissociator output should have first and second moments as low as possible. Besides high dissociation efficiency and narrow, low-average velocity distributions, other important considerations for the design of space-qualified hydrogen dissociators are low power consumption and low wall recombination rates during the lifetime of the maser.

We have performed theoretical studies of two types of dissociators: RF discharge, and thermal. In the RF discharge type, hydrogen mole-

cules are dissociated by spin-exchange collisions with energetic electrons (E > 8.5 eV) in the discharge-generated low-density plasma. High atomic fractions can be achieved easily at moderate discharge power. In the thermal type, hydrogen molecules dissociate on a hot tungsten surface. Reasonable atomic fractions can be achieved, but the radiative power losses are high. For both types of dissociators it is difficult to predict the speed distributions of the H atoms in the output beam, since in both cases the atoms have initially some excess energy and, due to the conditions under which the dissociators are operated, it is not clear whether they will reach thermal equilibrium with the walls before leaving or not.

In order to evaluate atomic fractions and speed distributions for both types of dissociators we have built an atomic beam apparatus consisting of a hydrogen purifier and controlled leak, an atomic source (i.e., the dissociator under study) a dipole electromagnet with pole-pieces shaped to produce an inhomogeneous, magnetic field in the "two-wire" configuration, and two detectors which can be displaced normal to the beam: a pirani detector,[23] sensitive to both atomic and molecular hydrogen, and a heat-of-recombination detector,[24] which senses only atomic hydrogen. Fig. 16 shows schematically our experimental arrangement. When the magnet is turned on, atoms having opposite spin states are deflected in opposite directions, giving rise to a double-peaked intensity distribution in the detector plane. Careful measurements of the deflected beam intensity profiles will yield information on the atomic speed distribution. This apparatus has been tested and calibrated using Cs and Rb beams; Fig. 17 shows some deflected alkali beam intensity profiles. This facility can be of particular value in characterizing new dissociator designs.

III. CONCLUSIONS

The Aerospace Corporation's Chemistry and Physics Laboratory Atomic Clocks Program is composed of a number of specific tasks aimed at improving the performance and reliability of compact atomic frequency standards designed for use on USAF satellites. In order to develop and maintain the needed expertise, the tasks are distributed across a range of atomic standards. The areas in which effort is expended have been chosen such that the results will lead to improved performance and reliability of the standard with which the investigations are associated. The goal of this paper has been to further inform the time and frequency community of our investigations and foster communications between Aerospace and both military and civilian members of that community.

ACKNOWLEDGEMENTS

The authors would like to thank Mr. R. Cook, Mr. S. Delcamp and Mr. C. Kahla for their technical assistance in performing all aspects of the experimental work described above. This work is supported by the United States Air Force Space Division under contract No. F04701-85-C-0086.

REFERENCES

1) J. Vanier, "Relaxation in Rubidium-87 and the Rubidium Maser," Phys. Rev. 168, 129 (1968); G. Missout and J. Vanier, "Some Aspects of the Theory of Passive Rubidium Frequency Standards," Can. J. Phys. 53, 1030 (1975).

2) J. C. Camparo and R. P. Frueholz, "Linewidths of the 0-0 Hyperfine Transition in Optically Pumped Alkali-Metal Vapors," Phys. Rev. A 31, 1440 (1985); J. C. Camparo and R. P. Frueholz, "Saturation of the 0-0 Hyperfine Transition Linewidth Enhancement Factor in Optically Pumped Alkali-Metal Vapors," Phys. Rev. A 32, 1888 (1985).

3) J. C. Camparo and R. P. Frueholz, "A Nonempirical Model of the Gas-Cell Atomic Frequency Standard," J. Appl. Phys. 59, 301 (1986).

4) R. P. Frueholz and J. C. Camparo, "Microwave Field Strength Measurement in a Rubidium Clock Cavity via Adiabatic Rapid Passage," J. Appl. Phys. 57, 704 (1985).

5) P. Minguizzi, F. Strumia and P. Violino, "Temperature Effects in the Relaxation of Optically Oriented Alkali Vapors," Nuovo Cimento 46B, 145 (1966).

6) J. C. Camparo and R. P. Frueholz, "Fundamental Stability Limits for the Diode-Laser-Pumped Rubidium Atomic Frequency Standard," J. Appl. Phys. 59, 3313 (1986).

7) J. Vanier and L-G Bernier, "On the Signal-to-Noise Ratio and Short-Term Stability of Passive Rubidium Frequency Standards," IEEE Trans. Instrum. Meas. IM-30, 277 (1981).

8) J. C. Camparo and R. P. Frueholz, "A Comparison of Various Alkali Gas Cell Atomic Frequency Standards," to be published in IEEE Trans. Ultra. Ferro. and Freq. Contrl.

9) J. C. Camparo, "A Partial Analysis of Drift in the Rubidium Gas Cell Atomic Frequency Standard," submitted to IEEE Trans. Ultra. Ferro. and Freq. Contrl.

10) A. Risely and G. Busca "Effect of Line Inhomogeneity on the Frequency of Passive Rb^{87} Frequency Standards," Proc. 32nd Annual Symp. on Freq. Control (Electronic Industries Assoc., Washington, D.C., 1978) pp. 506-513; A. Risely, S. Jarvis, Jr., and J. Vanier, "The Dependence of Frequency Upon Microwave Power of Wall-Coated and Buffer-Gas-Filled Gas Cell Rb^{87} Frequency Standards," J. Appl. Phys. 51, 4571 (1980).

11) J. C. Camparo, R. P. Frueholz and C. H. Volk, "Inhomogeneous Light Shift in Alkali-Metal Atoms," Phys. Rev. A 27, 1914 (1983).

12) T. McClelland, L. K. Lam, T. M, Kwon, "Anomalous Narrowing of Magnetic-Resonance Linewidths in Optically Pumped Alkali-Metal Vapors," Phys. Rev. A 33, 1697 (1986).

13) A. Kastler, "Displacement of Energy Levels of Atoms by Light," J. Opt. Soc. Am. 53, 902 (1963).

14) L. C. Balling, "Optical Pumping," in Advanced in Quantum Electronics, vol. 3, (Academic Press, London, 1975).

15) N. F. Ramsey, Molecular Beams (Oxford University Press, London, 1956).

16) L. W. Anderson and A. T. Ramsey, "Study of the Spin-Relaxation Times and the Effects of Spin Exchange Collisions in an Optically Oriented Sodium Vapor," Phys. Rev. 132, 712 (1963).

17) C. H. Volk, R. P. Frueholz, T. C. English, T. J. Lynch and W. J. Riley, "Lifetime and Reliability of Rubidium Discharge Lamps For Use in Atomic Frequency Standards," Proc. 38th Annual Symp. Freq. Control. (IEEE Press, New York, 1984) pp. 387-400.

18) R. P. Frueholz, M. Wun-Fogle, H. U. Eckert, C. H. Volk and P. F. Jones, "Lamp Reliability Studies for Improved Satellite Rubidium Frequency Standards," Proc. 13 Annual Precise Time and Time Interval (PTTI) Applications and Planning Meeting (NASA Conference Publication 2220, 1982) pp. 767-790.

19) E. G. Nazarov, "Observataion of Atomic Desorption Dynamics with a Voltage-Modulation Method," Zh. Tekh. Fiz. (USSR) 49, 1277 (1979); Transl: Sov. Phys. Tech. Phys. 24, 707 (1979).

20) M. A. Bouchiat, "Releaxation Magnetique d'Atomes de Rubidium sur des Parois Paraffines," J. Phys. (Paris) 24, 379 (1963).

21) S. Wexler, "Deposition of Atomic Beams," Rev. Mod. Phys. 30, 402 (1958).

22) D. Kleppner, H. M. Goldenberg and N. F. Ramsey, "Theory of the Hydrogen Maser," Phys. Rev. 126, 603 (1962).

23) A. G. Prodell and P. Kusch, "The Hyperfine Structure of Hydrogen and Deuterium," Phys. Rev. 88, 184 (1952).

24) K. C. Harvey and C. Fahrenbech, Jr., "Semiconductor Detector for the Selective Detection of Atomic Hydrogen," Rev. Sci. Instrum. 54, 1117 (1983).

	Rb	Cs	H-MASER
RELIABILITY ORIENTED	LAMP STUDIES	ELECTRON MULTIPLIERS GRAPHITE GETTERING Cs OVEN DESIGN	H-DISSOCIATOR
PERFORMANCE ORIENTED	FREQUENCY DRIFT CLOCK MODEL OPTICAL PUMPING	OPTICAL PUMPING ERROR SIGNAL DISTORTIONS	H-DISSOCIATOR HYPERFINE MOTIONAL NARROWING

Figure 1: Overview of topics currently under investigation in the Aerospace Corporation Chemistry and Physics Laboratory.

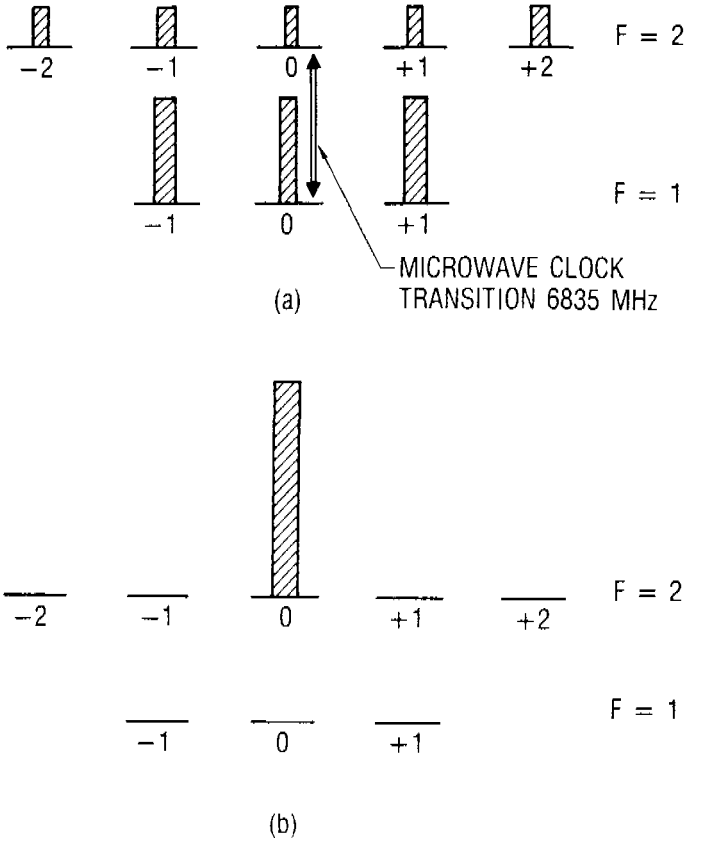

Figure 2: a) Schematic representation of the typical atomic hyperfine polarization generated in Rb gas cell atomic clocks. Shaded rectangles represent population amplitudes n(F,m). b) Concentration of all the atoms in single m=0 Zeeman sublevel.

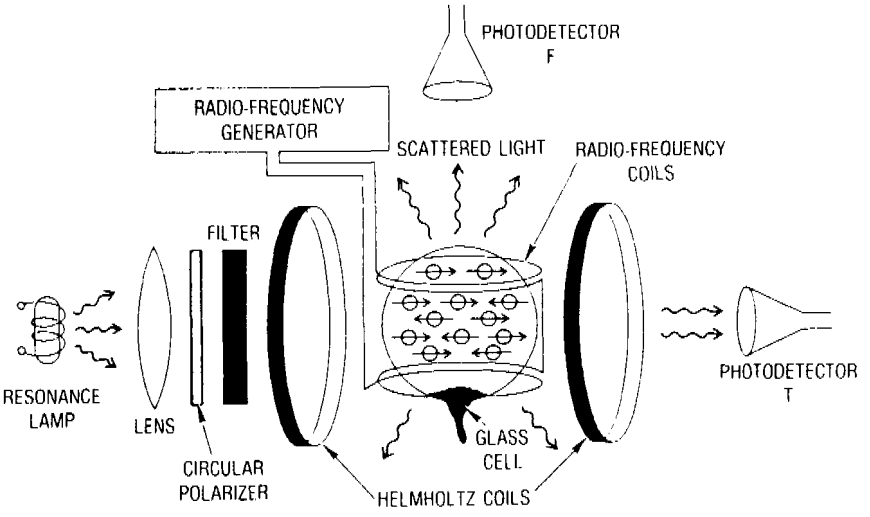

Figure 3: Schematic of the apparatus used for studying the population distributions among the ground state Zeeman sublevels in an optically pumped Rb vapor.

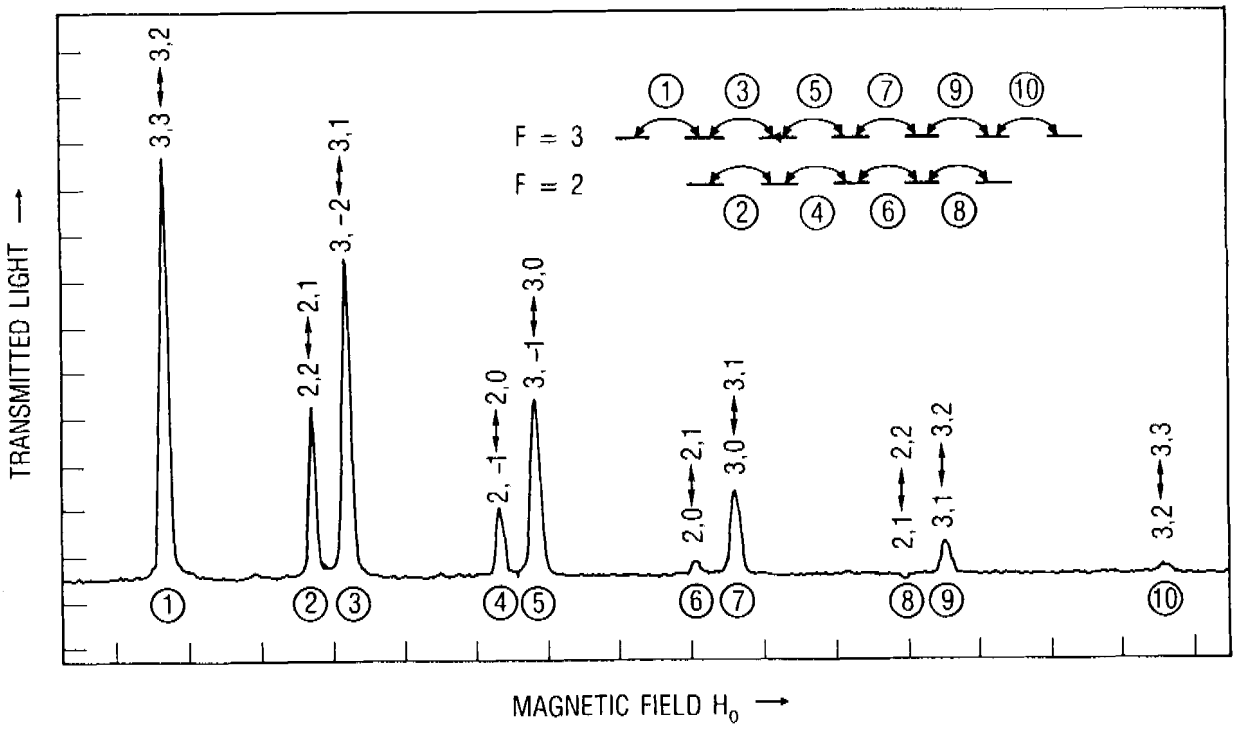

Figure 4: Typical experimental data for rf transitions (F,m) - (F, m-1) for Rb^{85} (I=5/2) in a vapor cell containing natural Rb. The signal amplitude is proportional to the population difference Δn.

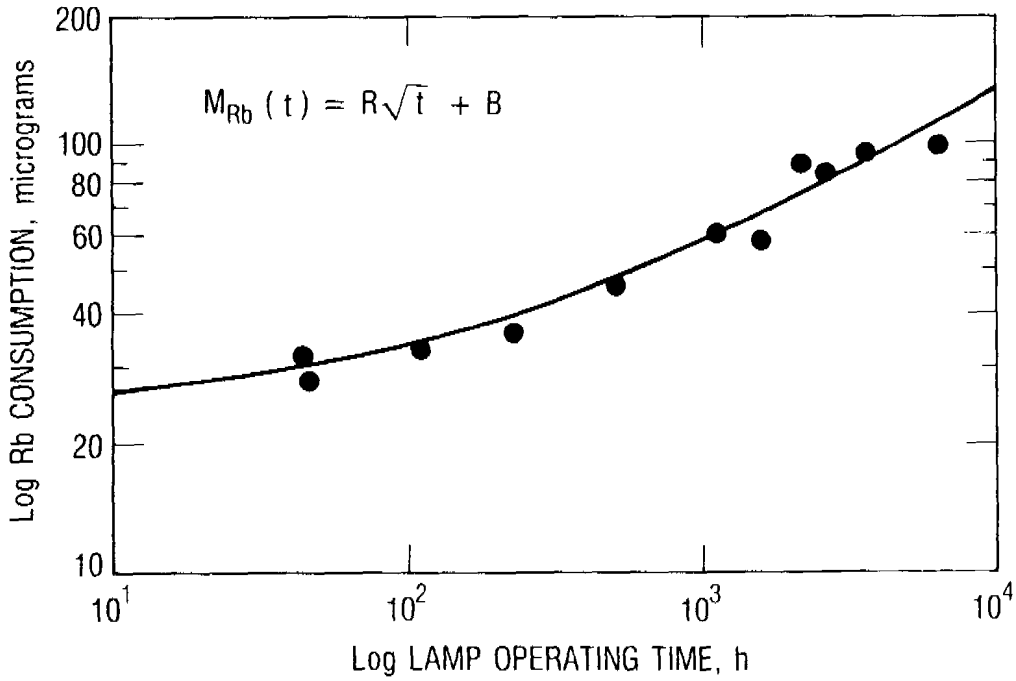

Figure 5: Typical Rb consumption data for a discharge lamp operating under normal conditions. The solid line represents a fit to the diffusion law indicated on the figure.

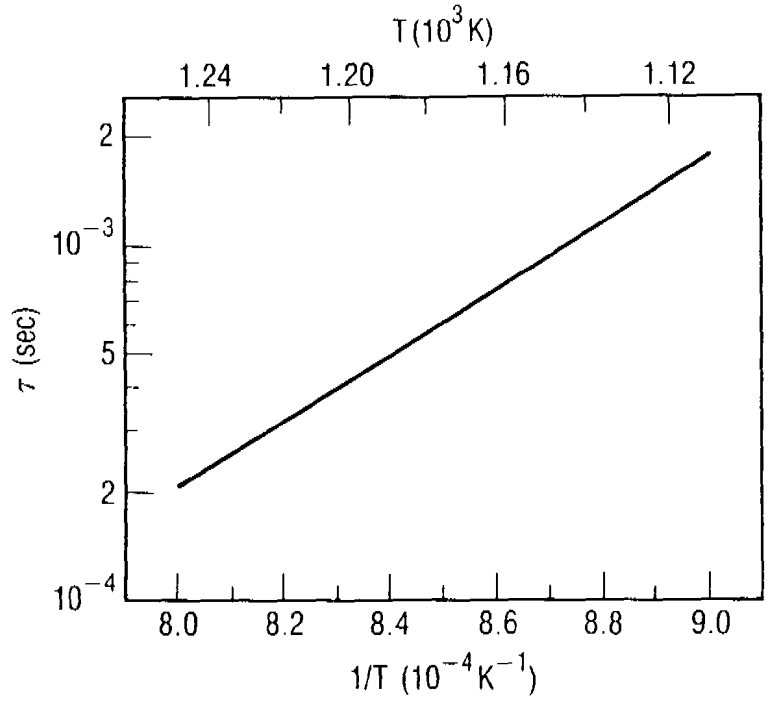

Figure 6: Cesium ionic dwell time on polycrystalline tungsten vs. temperature following Nazarov (Ref. 19).

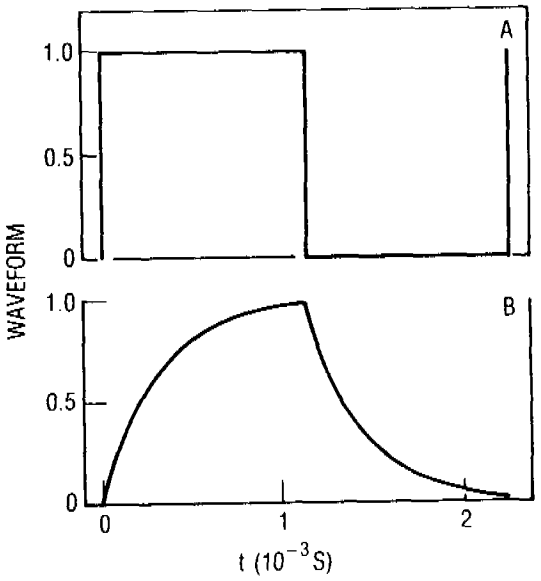

Figure 7: Waveforms (in arbitrary units) for a single-velocity cesium beam incident on a tungsten ionizer: $f \tilde{=} 500$ Hz, τ $3x10^{-4}$ sec. Figure 7a is the incident atomic beam and Fig. 7b is the emerging ion current.

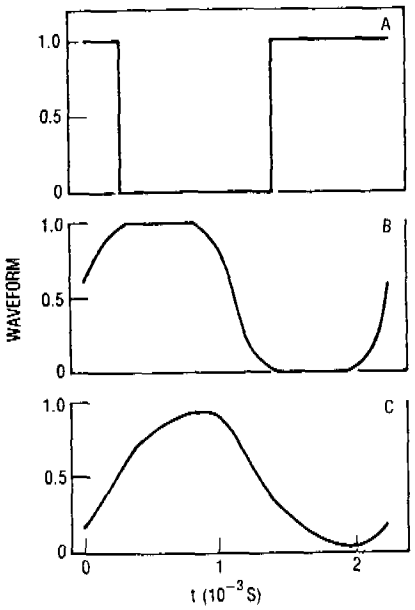

Figure 8: Waveforms (in arbitrary units) for a cesium beam with a gaussian velocity distribution that is incident on a tungsten ionizer: $\bar{t}_A = 1.4x10^{-3}$ sec., $\bar{v} \tilde{=} 120$ m/sec., $\sigma = 10$m/sec., $f \tilde{=} 500$ Hz, τ $3x10^{-4}$ sec. Figure 8a is the atomic beam at the point of modulation; Fig. 8b is the atomic beam arriving at the ionizer, and Fig. 8c is the emerging ion current.

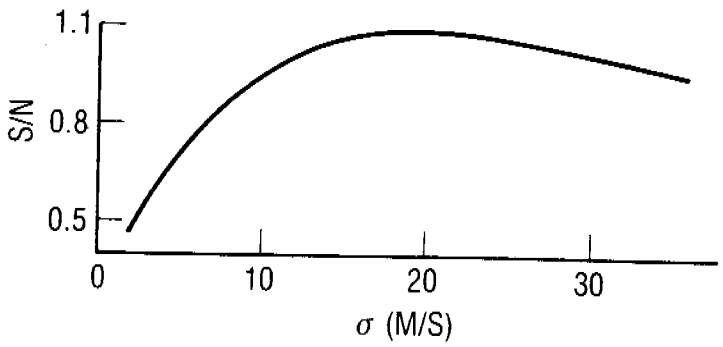

Figure 9: Signal-to-noise ratio (in arbitrary units) vs. the width of the atomic velocity distribution, which is assumed to be a gaussian of standard deviation σ: $\bar{v} \approx 120$ m/sec., $\bar{t}_A = 1.4 \times 10^{-3}$ sec., $f \approx 500$ Hz, and $\tau = 3 \times 10^{4}$ sec.

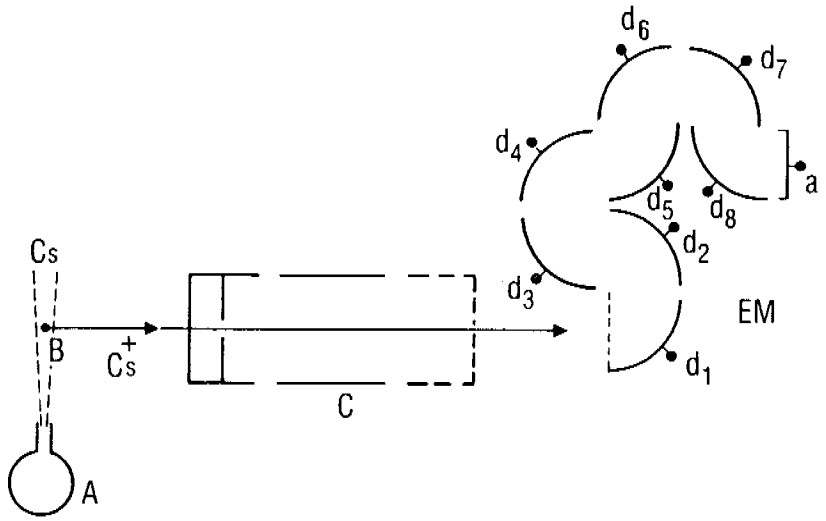

Figure 10: Electron multiplier test bed schematic: A is the cesium oven; B is the hot-wire ionizer; C is the Einzel lens and steering electrodes; EM is the electron multiplier; d_i is the i-th dynode and a is the anode.

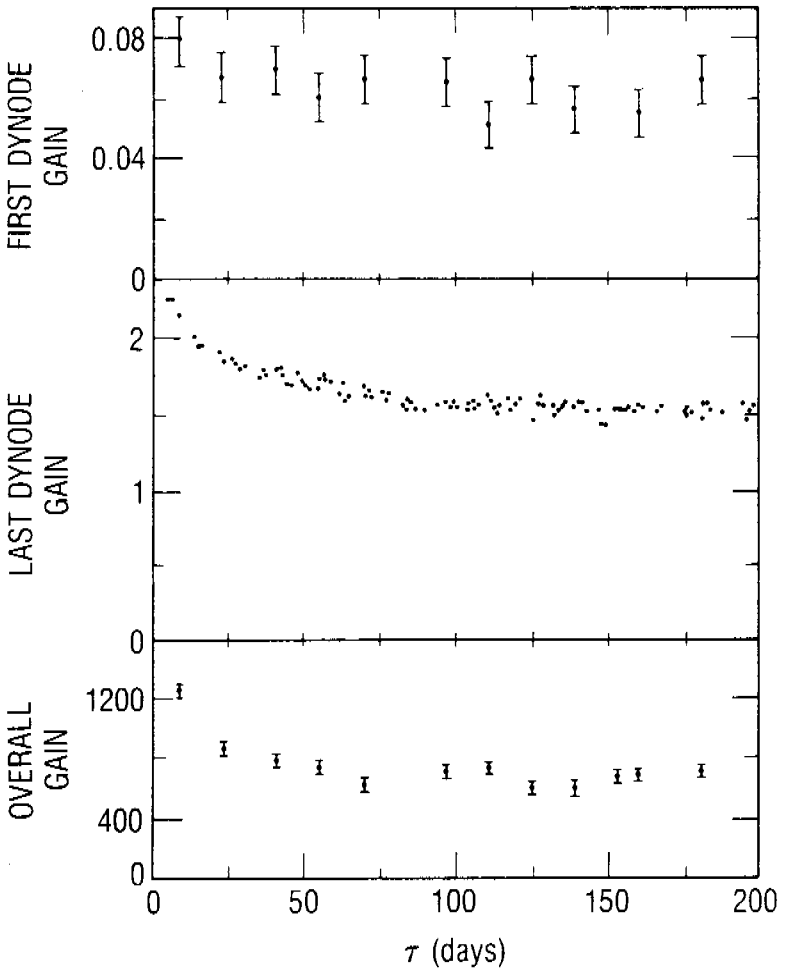

Figure 11: First dynode, last dynode and overall gain versus time for a GPS-type electron multiplier under test.

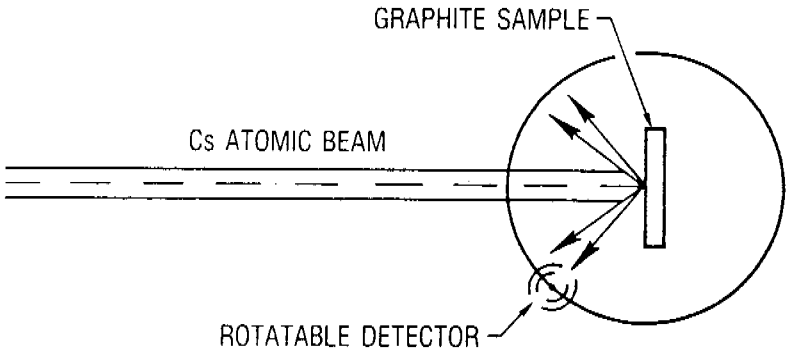

Figure 12: Schematic of the experimental arrangement used for the measurement of the sticking coefficient γ for Cs on graphite. For reference the graphite sample is replaced with paraffin coated surface.

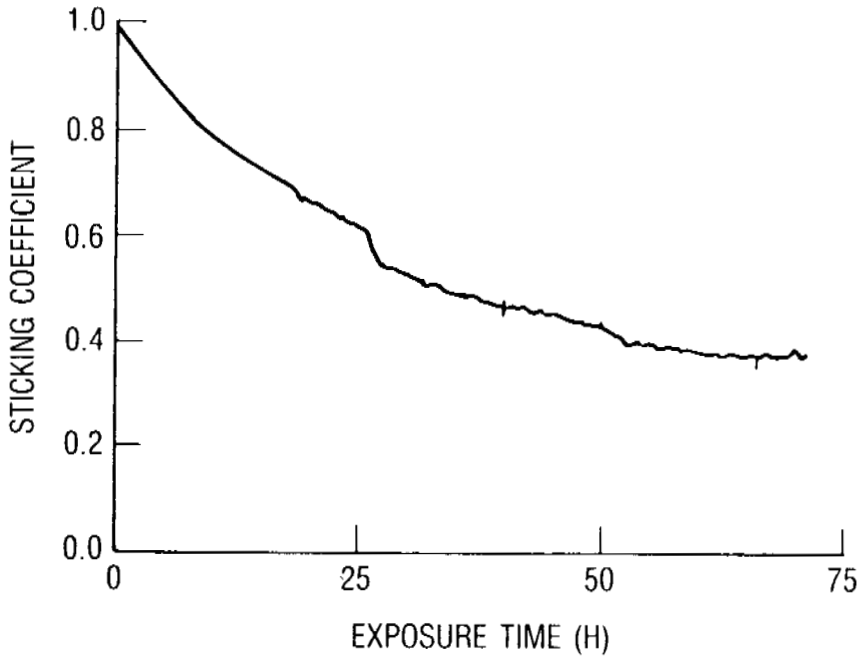

Figure 13: Experimental data showing the decline of γ with exposure time. The cesium beam flux incident of the POCO CZR-R graphite sample was 6.2×10^{11} atoms/cm^{2}s.

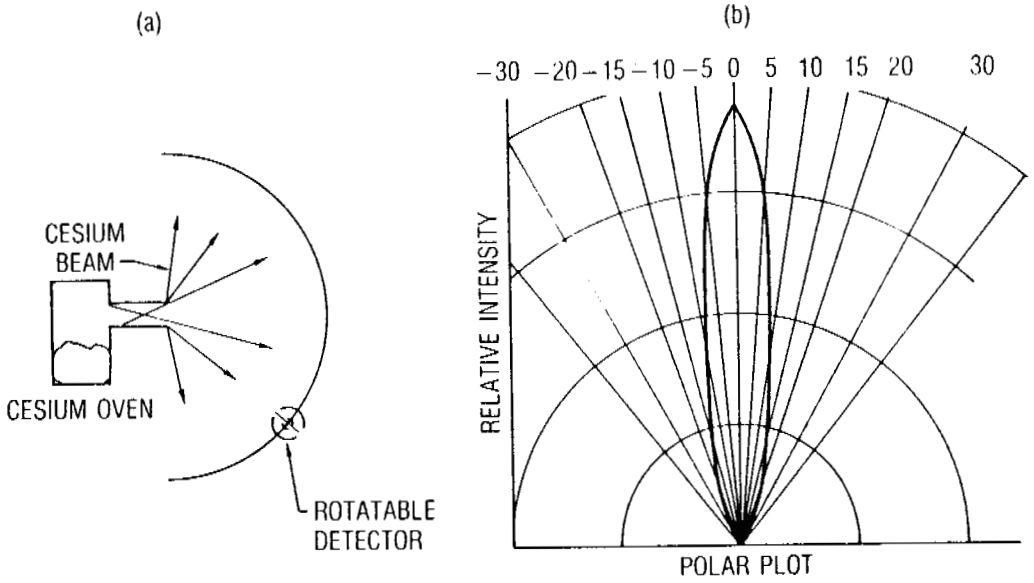

Figure 14: a) Schematic of the apparatus employed to measure the angular distribution of atoms emitted from a cesium oven. b) Experimental data yielded by the apparatus plotted in terms of the detected intensity versus polar angle.

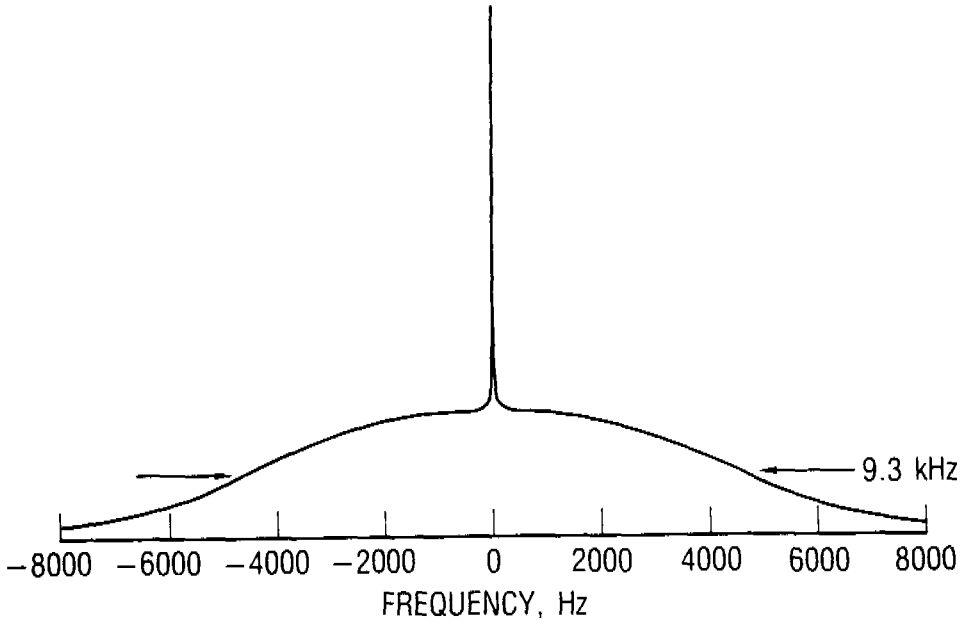

Figure 15: Dicke-narrowed hyperfine lineshape obtained from a trajectory/density matrix analysis. Initial experimental and theoretical analyses have been performed on Rb^{87}.

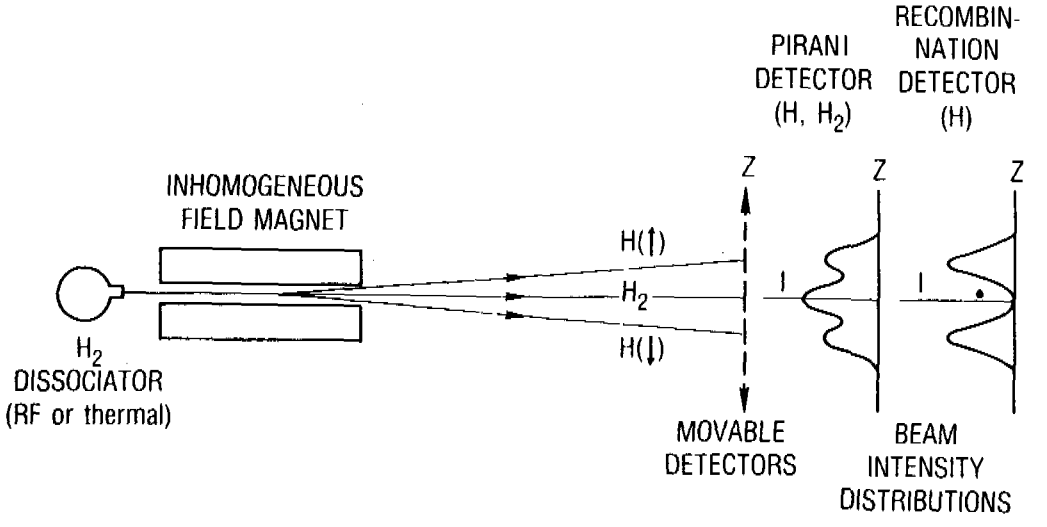

OBJECTIVES: TO MEASURE DISSOCIATION FRACTIONS, AVERAGES AND WIDTHS OF VELOCITY DISTRIBUTIONS

Figure 16: a) Schematic of the experimental arrangement for determining the velocity distribution of H-atoms emitted by the H-atom dissociator. The dashed lines give trajectories of molecular hydrogen (center) and atomic hydrogen with spin up and down when the "two-wire" field magnet is turned on. Figure 16b shows the expected intensity distributions. I_0 is magnet off; I_1 is magnet on an measured by recombination detector, and I_2 is magnet on but measured with the Pirani detector.

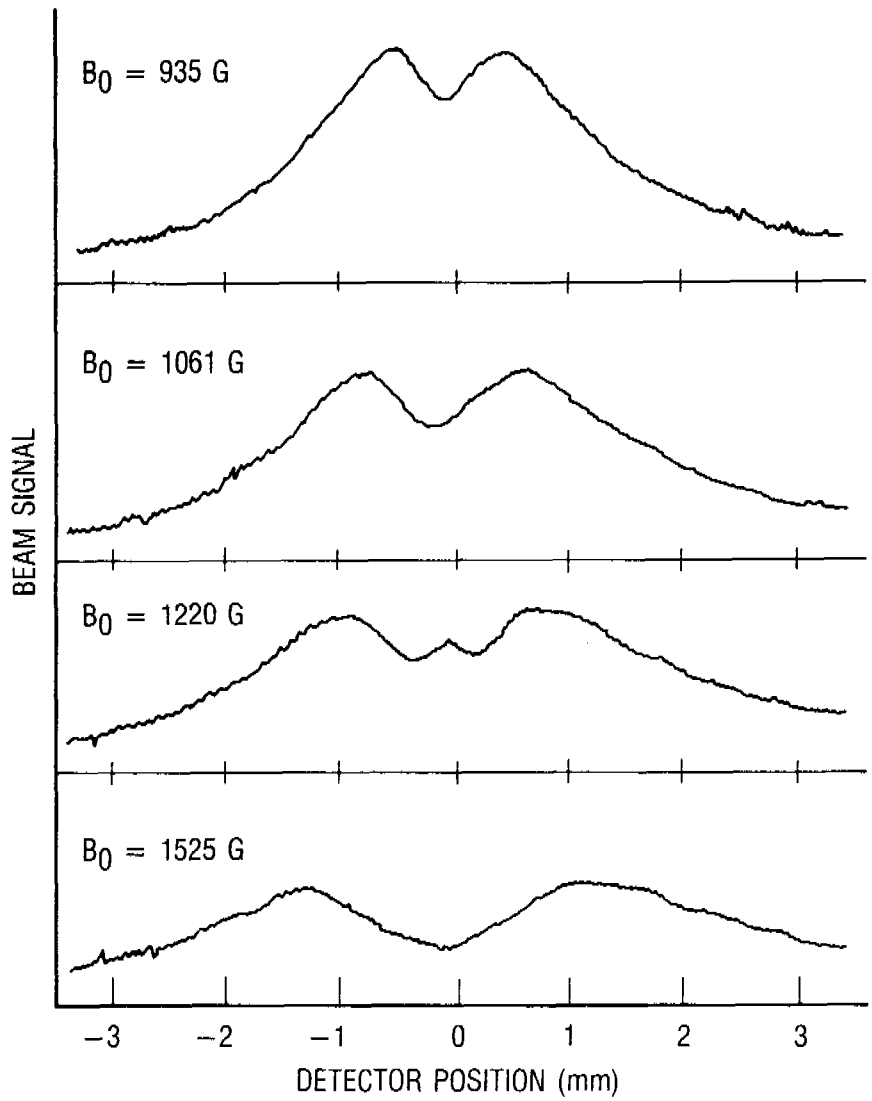

Figure 17: Rubidium atomic beam intensity profiles after deflection in the "two-wire" field magnet; fields are given in gauss. The central features at B_o - 1220 G is the signature of the m = - 1 states, which have zero effective magnetic moment at that field strength.